Published in final edited form as:
Proteomics. 2009 April ; 9(7): 1925–1938. doi:10.1002/pmic.200800118.

Proteomic Analysis of Low Dose Arsenic and Ionizing Radiation Exposure on Keratinocytes

Susanne R. Berglund[1,*], **Alison R. Santana**[2], **Dan Li**[3], **Robert H. Rice**[4], **David M. Rocke**[5], and **Zelanna Goldberg**[6]

1*Siemens Healthcare Diagnostics, 1584 Enterprise Blvd, West Sacramento, CA, USA, 95691*

2*Public Health Sciences, University of California Davis, 1 Shields Ave, TBS 168, Davis, CA, USA, 95616*

3*Graduate Group in Applied Mathematics, University of California Davis, Davis, 1 Shields Avenue, CA, USA, 95616*

4 *Department of Environmental Toxicology, University of California Davis, 1 Shields Ave, 4243 Meyer Hall, Davis, CA, USA, 95616*

5*Division of Biostatistics, University of California Davis, 1 Shields Avenue, Davis, CA, USA, 95616*

6*Oxigene Inc., 1001 Bayhill Drive, Suite 200, San Bruno, CA 94066*

Abstract

Human exposure to arsenic and ionizing radiation occur environmentally at low levels. While the human health effects of arsenic and ionizing radiation have been examined separately, there is little information regarding their combined effects at doses approaching environmental levels. Arsenic toxicity may be affected by concurrent ionizing radiation especially given their known individual carcinogenic actions at higher doses. We found that keratinocytes responded to either low dose arsenic and/or low dose ionizing radiation exposure, resulting in differential proteomic expression based on 2DGE, immunoblotting and statistical analysis. Seven proteins were identified that passed a rigorous statistical screen for differential expression in 2DGE and also passed a strict statistical screen for follow-up immunoblotting. These included: α-enolase, epidermal-fatty acid binding protein, heat shock protein 27, histidine triad nucleotide-binding protein 1, lactate dehydrogenase A, protein disulfide isomerase precursor and S100A9. Four proteins had combined effects that were different than would be expected based on the response to either individual toxicant. These data demonstrate a possible reaction to the combined insult that is substantially different from that of either separate treatment. Several proteins had different responses than what has been seen from high dose exposures, adding to the growing literature suggesting that the cellular responses to low dose exposures are distinct.

Keywords

arsenic; human; ionizing radiation; keratinocyte; low dose

*Corresponding author: Susanne Berglund, Siemens Healthcare Diagnostics 1584 Enterprise Blvd, West Sacramento, CA, USA 95691; sberglund@ucdavis.edu Phone: (916) 374-2223; Fax: (916) 375-8673

Conflict of Interest Statement: All authors declare that there are no conflicts of interest

Introduction

Low level arsenic and low dose ionizing radiation are both environmental toxicants. While data exist which examine the human health effects of either toxicant separately, there are no data in the literature regarding possible combined effects at low doses. Yet, combined effects of toxicants to produce disease are a well-known phenomenon (e.g. radon and/or arsenic with tobacco smoke induce lung cancer) [1,2]. In the context of human health, the potential effects of receiving combined or sequential exposure to these particular toxicants in a medical setting requires further biologic characterization. The FDA has approved the use of arsenic to treat acute promyelocytic leukemia, while the growing use of intensity modulated radiation therapy to treat a wide variety of cancer has resulted in increasing amounts of healthy tissue being exposed to low dose ionizing radiation (LDIR) [3,4]. Low dose arsenic toxicity may be affected by concurrent ionizing radiation especially in light of their known carcinogenic actions individually at higher doses [3,5].

Arsenic is a naturally occurring metalloid that can be solubilized in water, posing the threat of contaminated drinking water [5]. It has been well documented that exposure to arsenic can contribute to skin, bladder, liver and lung cancers [6]. While the mechanisms of arsenic toxicity are not fully understood, several ideas include the induction of oxidative stress, decreased functioning of DNA repair systems, chromosomal abnormality and altered growth factors [6-10]. There is evidence that exposure to arsenic generates an oxidative stress response, increasing reactive oxygen species (ROS) which can mutate and/or damage DNA [9,11]. A change in expression of genes involved in the synthesis of DNA repair enzymes has been proposed as an explanation to arsenic's co-mutagenic effects [12,13].

Ionizing radiation (IR) exposure is unavoidable in the environment and further exposure is obtained through medical imaging. There is substantial debate regarding the biological effects of LDIR in humans and no direct information on how such exposure may alter the response of cells to other environmental toxicants [14]. As with arsenic, IR exerts the majority of its toxicity through the intracellular generation of ROS [15]. It is plausible that oxidative stress induced from IR could substantially enhance the effects of otherwise minimally toxic, sub-lethal exposures of arsenic.

Much remains uncertain about the effects of these toxicants at low doses. Historically, radiation and arsenic studies have involved high dose exposures with the assumption that the toxicant profile could be extrapolated down in a linear manner for low dose exposures. This is the underlying assumption in the linear no-threshold model of radiation effects, which is currently undergoing challenge [16]. Likewise, much remains unknown about the dose response curve for low level arsenic exposure. Again, it was assumed that the response for high doses of arsenic could also be applied to low dose exposures [5]. However, current studies have yet to demonstrate a direct relationship between low dose arsenic exposure and cancer, suggesting a nonlinear relationship and supporting the idea that the dose response curve at low levels cannot be inferred from high dose studies [17,18]. Thus, as there is no accepted, comprehensive model describing the mechanism by which low dose toxin exposures exert their effects, there is no predictive modeling that can address the potential interacting effects of co-exposures on cells. Therefore, direct empiric study remains the cornerstone of understanding potential interactions and how the co-exposures may alter the safety profile of each.

It has been shown that transcriptional changes within the cell do not correlate completely with translational data [19,20]. Few studies have focused on the proteomic differences induced by these toxicants [21,22]. As proteins are the molecules through which a cell enacts change, the differences found in the proteome may better reflect the actual cellular response. Using a

proteomics approach in a human keratinocyte model to mimic human skin exposure, we examined the interaction of IR and arsenic.

Materials and Methods

Cell Culture

A spontaneously immortalized human keratinocyte cell line was grown in T-75 cm^2 tissue culture flasks with a lethally irradiated feeder layer of 3T3 cells obtained from ATCC #48-X (ATCC, VA). Cells were supported with a 3:1 mixture of Dulbecco-Vogt Eagle and Ham's F-12 medium with the addition of serum and other factors as previously described [23].

Arsenic and IR Treatment

Once cells reached near confluency, half of the flasks were treated with medium containing 2 μM sodium arsenite. At 24 hours, flasks were irradiated with a Varian 2100C linear accelerator on a 30 × 30 cm^2 solid water block covered with a tissue equivalent bolus to ensure accuracy of dose delivery. Dose rate was set at 80 cGy/min, and SSD was 101.3 cm (1 cGy) or 100 cm (10 cGy). Radiation free controls were maintained with and without sodium arsenite. One or four days post irradiation, flasks were rinsed with 0.02% EDTA in phosphate buffered saline to remove residual 3T3 cells and held at −80° C until protein extraction. All samples were prepared in triplicate.

Protein Extraction

One ml of Mammalian Protein Extraction Reagent (Pierce Biotechnology, IL) containing protease inhibitor (Sigma-Aldrich, MO) was added to each flask, cells were scraped and lysate transferred to a 2 ml tube on ice. Each sample was sonicated for 1 minute and centrifuged at 10,000 × *g* for 20 minutes at 4°C. Supernatant was removed and placed in a clean 2 ml tube. Protein quantitation was performed using Coomassie Plus Protein Assay (Pierce Biotechnology, IL).

2D electrophoresis

Isoelectric focusing was performed using a Protean IEF Cell (Bio-Rad, CA). 30 μg of protein was combined with lysis solution (0.5% Triton X-100, 4% CHAPS, 7 M urea, 2 M thiourea, nanopure water), 1% Biolyte 3-10 buffer, 2% protease inhibitor cocktail (Calbiochem, CA), 0.065% ditheothreitol and a trace amount of bromophenol blue dye for a total volume of 200 μl. The protein samples were left at room temperature for one hour before loading. ReadyStrip IPG strips (pH 3-10, 11cm) were used for separation (Bio-Rad, CA).

Isoelectric focusing was conducted at 20°C using the following program: 50 V for 12- hours; 50-250 V linear ramp; 250-8000 V linear ramp and hold for a total of 42 kVh. After focusing, the strips were incubated in an equilibration buffer (5 ml consisting of 50 mM Tris, pH 8.8, 6 M urea, 30% glycerol, 2% SDS, trace bromophenol blue and 0.065% ditheothreitol (DTT)) for 15 minutes on a rocking platform. The strips were subsequently incubated with the same equilibration buffer substituting 10 mM iodoacetamide for DTT to alkylate cysteine sulfhydryls. Each strip was then placed on top of a 12% SDS Duracryl gel and sealed using 0.5% agarose (Genomic Solutions, MI).

The second dimension separation was performed in a Hoefer SE 600/SE 660 2D-PAGE system. Gels were run in buffer (25 mM Tris, 192 mM glycine, 0.1% SDS) at 15 mA per gel for 30 minutes followed by 25 mA per gel until the dye migrated to the bottom of the gel. Broad Range Precision Plus Protein Standard molecular weight protein plugs were used for mass calibration of the gels (10-250 kDa) (Bio-Rad, CA). Gels were fixed in 10% acetic acid, 40%

methanol, and 50% water, silver stained and scanned with an Epson Perfection 4870 photo scanner.

Image analysis

The 36 gel images were processed with the analysis software Progenesis (PG240 v2006) and TT900 S2S (Nonlinear Dynamics, UK). Gel images were first warped with TT900 S2S. Warped images were then imported to Progenesis for further analysis including: spot detection, spot matching, background subtraction, spot filtering and 'Samespot Outline'. The Samespot Outline in Progenesis copies spot outlines from gels where a spot exists to those gels missing the spot, then calculates the spot volume within the new outlines. Therefore all missing values are filled with calculated volumes.

Protein digestion and mass spectrometry

The Nevada Proteomics Center analyzed selected proteins using MALDI TOF/TOF analysis. Spots were destained and digested using a previously described protocol with some modifications [24]. Samples were washed twice with 25 mM ammonium bicarbonate (ABC) and 100% acetonitrile, reduced and alkylated using 10 mM DTT and 100 mM iodoacetamide and incubated with 75 ng sequencing grade modified porcine trypsin (Promega, WI) in 25 mM ABC for 6 hours at 37°C. Samples were spotted onto a MALDI target with ZipTip μ-C18 (Millipore Corp., MA). Samples were eluted with 70% acetonitrile, 0.2% formic acid and overlaid with 0.5 μl 5 mg/ml MALDI matrix (α-Cyano-4 hydroxycinnamic acid, 10 mM ammonium phosphate). All mass spectrometric data were collected using an ABI 4700 Proteomics Analyzer MALDI TOF/TOF mass spectrometer (Applied Biosystems, CA), using their 4000 Series Explorer software v. 3.6. The peptide masses were acquired in reflectron positive mode (1-keV accelerating voltage) from a mass range of 700 – 4000 Daltons and either 1250 or 2500 laser shots were averaged for each mass spectrum. Each sample was internally calibrated on trypsin's autolysis peaks 842.51 and 2211.10 to within 20 ppm. Any sample failing to internally calibrate was analyzed under default plate calibration conditions of 150 ppm. Raw spectrum filtering/peak detection settings were S/N threshold of 3, and cluster area S/N optimization enabled at S/N threshold 10, baseline subtraction enabled at peak width 50. The eight most intense ions from the MS analysis, which were not on the exclusion list, were subjected to tandem mass spectrometry. The MS/MS exclusion list included known trypsin masses along with unidentified background peaks: 842.51, 856.52, 870.54, 1011.65, 1045.56, 1126.56, 1338.83, 1666.01, 1794.9, 1940.94, 2211.10, 2225.12, 2283.18 and 3094.62. For MS/MS analysis the mass range was 70 to precursor ion with a precursor window resolution of 50 FWHM (full-width at half maximum) with an average 2500 laser shots for each spectrum, CID on, metastable suppressor on. Raw spectrum filtering/peak detection settings were S/N threshold of 5, and cluster area S/N optimization enabled at S/N threshold 6, baseline subtraction enabled at peak width 50. The data was then stored in an Oracle database (Oracle database schema v. 3.19.0, Data version 3.90.0).

MALDI data analysis

The data was extracted from the Oracle database and a peak list was created by GPS Explorer software v 3.6 (Applied Biosystems). Analyses were performed as combination mass spectrometry and tandem mass spectrometry. MS peak filtering included mass range 700-4000 Da, minimum S/N filter 10, mass exclusion tolerance of 0.2 Da. Exclusion list of known trypsin fragments and unidentified background peaks: 2211.2, 2283.2, 1045.6, 842.5, 1794.9, 1011.65, 1338.83 and 1666.01. A peak density filter of 50 peaks per 200 Da with a maximum number of peaks set to 65. MS/MS peak filtering included mass range of 60 Da to 20 Da below each precursor mass. Minimum S/N filter 5, peak density filter of 50 peaks per 200 Da, cluster area filter used with maximum number of peaks 65. The filtered data were searched by Mascot v.

1.9.05 (Matrix Science) using CDS combined database (Celera Discovery System v. KBMS3.2.20040119), containing 1,416,555 sequences. Searches were performed without restriction to protein species, Mr, or pI and with variable oxidation of methionine residues and carbamidomethylation of cysteines (no fixed modifications). Maximum missed cleavage was set to 1 and limited to trypsin cleavage sites. Precursor mass tolerance and fragment mass tolerance were set to 20 ppm and ± 0.2 Da, respectively. Protein hits with high confidence identifications and statistically significant search scores, greater than 95% confidence interval (C.I.%) or $p \leq 0.05$, were accepted. The majority of the ions present in the mass spectra were accounted for and high confidence identifications were consistent with the protein experimental Mr, and pI.

Immunoblot analysis

10 μg of each sample were separated on 12%, Ready Gel Tris-HCl precast gels (BioRad, CA), transferred to PVDF and blocked overnight at 4°C. The primary antibodies included: pyruvate kinase (ab6191, Abcam, MA), α-enolase (sc-15343, Santa Cruz Biotechnology, CA), S100A9 (sc-8114), PDI (sc-30932), profilin-1 (sc-18346), annexin XI (sc-9322), E-FABP (sc- 16060), LDH-A (sc-27230), cytokeratin 1 (sc-17091), CaM (sc-1989), HSP27 (sc-1048), HINT-1 (10717-1-AP, Proteintech Group, IL) and cyclophilin A (10720-1-AP, Proteintech Group , IL). All primary antibodies were used at 0.2 μg/ml final concentration, typically a 1:1000 dilution. The secondary antibody (donkey anti-goat-HRP, sc-2020 or donkey anti-rabbit-HRP, sc-2004) was used at a 1:40,000 dilution. Membranes were developed using ECL Advanced (GE Healthcare, NJ) and images were captured on a ChemiDoc system with Quantity One software (BioRad, CA). A monoclonal antibody to β-actin was used as a loading control and all density readings were normalized (sc-47778). All western blots were performed in triplicate. The western blot data were analyzed using ANOVA in the R statistical software package after normalization by β-actin.

Statistical Analysis on 2D Gels

For each spot aligned across gels, the image analysis produces a spot volume, either directly or from the Same Spot method of imputation. We took the natural logarithms of the spot volumes and then used additive mean normalization. We then used two-way ANOVA with interaction on each spot to identify differentially expressed proteins with effects for the level of arsenic, the level of IR, and the interaction effect. Two methods of estimating the protein-specific variance in ANOVA were utilized, the usual mean square for error and an estimate adjusted by an empirical Bayes method originally developed for microarrays [25,26] (manuscript submitted, Dan Li, et al). The resulting p-values were adjusted for multiple comparisons using the Benjamini-Hochberg False Discovery Rate (FDR) method [27].

Results

Image and Statistical Analysis

Proteins were isolated from keratinocytes exposed to 0 or 2 μM sodium arsenite and 0, 1 or 10 cGy of irradiation for one or four days. These proteins were separated using two-dimensional gel electrophoresis. All conditions were run in triplicate and the resulting 36 gels were imaged and analyzed using Progenesis (PG240 v2006) and TT900 S2S (Nonlinear Dynamics, UK). The initial analysis included keratinocytes exposed to a 1 cGy dose. Little differential expression was detected with this low dose and these samples were omitted from further analysis, resulting in 24 remaining gels.

ANOVA was performed on each of the 2,002 spots detected separately at each time point. Thus, the ANOVA for each spot had 12 observations at each of two IR doses and each of two arsenic doses replicated in triplicate. Proteins that displayed significant differential expression

($p \leq 0.05$) after correction for multiple comparisons using either ANOVA method (see methods and materials) were selected as candidates for sequencing, resulting in 444 spots identified for further characterization.

Mass Spectrometry and Protein Identification

Protein spots were chosen for sequencing only if they were distinct, outside of areas with background smearing and could be removed from the gel without excising other nearby proteins. Most of the statistically significant spots did not meet these criterions, leaving 24 of the 444 available for identification.

A total of 24 samples were sent to the Nevada Proteomics Center for analysis, nine spots from day one and fifteen from day four. Thirteen proteins with protein score confidence indices above 95% were identified by mass spectrometry (MS) and tandem mass spectrometry (MS/MS) (table 1). The remaining proteins could not be identified with confidence. The proteins identified from the day one time point included: calmodulin (CaM), heat shock protein 27 (HSP27), lactate dehydrogenase A (LDH-A) and protein disulfide isomerase precursor (PDI, synonym: thyroid hormone binding protein precursor) (table 1). The proteins found four days post exposure included: annexin XI, S100A9 (synonym: calgranulin B), cyclophilin A (synonym: peptidyl-prolyl cis-trans isomerase), α-enolase, epidermal fatty acid binding protein (E-FABP), histidine triad nucleotide-binding protein 1 (HINT-1), profilin-1, pyruvate kinase M isozyme, and R3372_1 (protein fragment) (table 1).

Immunoblotting

Twelve identified proteins with available commercial antibodies were selected for immunoblotting to confirm significant differences between the control sample, IR only, arsenic only and IR with arsenic (figure 1). This was done as an important cross-check on the ANOVA analysis on the 2D gels. Given the complexity of the required statistical analysis for the 2D gels, it is always possible that some spots identified as differentially expressed were in fact artifactual. CaM was not recognized by the antisera in detectable amounts and no protein band was verified at the appropriate molecular weight. This does not exclude the possibility that CaM may have been differentially expressed since western blots require a relatively high concentration for detection.

ANOVA analysis

For the eleven proteins that had usable immunoblot data, the intensities were normalized to β-actin and these data were analyzed using ANOVA. The ANOVA analysis allows for direct comparison of a protein immunoblotted on independent gels by adjusting for density and background signal resulting in a more sensitive test. Seven of the eleven proteins (E-FABP, α-enolase, HINT-1, HSP27, LDH-A, PDI, and S100A9) showed significant ($p \leq 0.05$) differences for either IR, arsenic, or the interaction, which far exceeds the chance rate as roughly one or two false significance values could be expected out of the 11 proteins by chance alone (table 2). Four proteins (annexin XI, cyclophilin A, pyruvate kinase and profilin-1) showed no significant difference at the $p \leq 0.05$ level.

E-FABP, PDI and S100A9 decreased with exposure to arsenic. HSP27 was down-regulated and HINT-1 was up-regulated in response to individual treatments, neither protein showed an interaction effect that was significantly different than either single treatment. Four proteins showed a response to the combined insult that was different than would have been expected from either treatment alone. E-FABP and LDH-A showed an increased response while α-enolase and PDI had a response that was less than would have been expected based on the individual exposures.

Discussion

When below a certain threshold, the individual toxicity of IR and arsenic are believed to be minimal. However, the effects of combining these two known carcinogens at low doses are unknown. As a model for low dose toxicant interaction, they are of significant interest as irradiation is ubiquitous and arsenic, although heavily regulated in the U.S., is still a major environmental burden in many countries. There is little in the scientific literature examining human health risks associated with possible toxicant interactions despite the known roles of such agents in malignancy [2,6,8,28].

While the arsenic concentration used in this study is within environmental background levels (2 μM), the IR dose (10 cGy) is higher than the typical US average background exposure of 0.3 cGy per year. However, the natural background varies with location and Kerala Coast, India has a natural background of 1 cGy per year, while Ramsar, Iran receives 20 cGy per year. A single CT scan for medical purposes is 1 cGy, and the dose limits set by the DOE NCR for occupational exposure is 5 cGy (Office of Biological and Environmental Research, Office of Science, U.S. Department of Energy, Orders of Magnitude guide, March 2006). Higher exposures than these can occur occupationally, under medical treatment, or as a result of a nuclear accident.

The skin is the major barrier to many environmental toxicants, with keratinocytes being the most prevalent cell type. IR generally penetrates the skin, while arsenic exposure can lead to many diseases of the skin. Chronic arsenic exposure often leads to hyperpigmentation, hyperkeratosis and arsenic induced Bowen's disease [6]. In time, Bowen's disease can progress into invasive skin cancer in the form of basal or squamous cell carcinoma [6]. Keratinocytes, which have been used in previous sub-lethal arsenic and LDIR studies, are readily cultivated and respond to toxicant challenges with changes in transcription of up to 10% making them an ideal model for this study [23,29,30].

Of the twelve proteins selected for immunoblotting, seven showed significant differences in protein expression and four yielded inconsistent results (annexin XI, cyclophilin A, pyruvate kinase and profilin-1). It is possible that the expression changes detected by the ANOVA of the gel images were too small to be detected by western blotting given its semi-quantitative nature. All proteins with variable results had faint spots on the 2D gels indicating a very low protein concentration as silver staining can detect nanogram quantities of protein, a sensitivity beyond that of western blotting. Proteins that were immunoblotted included three proteins from the early time point: PDI, LDH-A and HSP27. None of these proteins were found at the later time point indicating a transient response. At four days post exposure, E-FABP, α-enolase, S100A9, and HINT-1 had altered expression. Doses examined in this study are much lower than those that are clearly cytotoxic and this proteomic response implies that the cells are actively responding to low-level exposures.

Both IR and arsenic dose responses are currently based on the idea of a linear no-threshold model [18,31]. Many studies are revealing that low dose exposures are fundamentally different from high dose exposures [17,31-34]. For example, it has been shown that α-enolase was up-regulated in-vivo with a high dose exposure of 9 Gy, whereas our low dose study showed the opposite expression [35]. Prasad et al showed that a high dose of 6 Gy of irradiation led to increases in the protein levels of PDI, calreticulin and calnexin in apoptotic cells 48 hours post exposure [36], whereas low dose exposure of 2 μM arsenic alone or with 10 cGy IR diminished cellular amounts of both PDI and calreticulin [23,36]. These results suggest that the response to low doses of irradiation and arsenic may be substantially different than those seen following higher dose exposures. A response pattern of that type would be consistent with emerging data from other studies dealing with LDIR and low dose arsenic [23,31-33].

Several of the identified proteins were found to have a response to the combined exposure that was different from the response to either toxicant individually, including E-FABP, α-enolase, LDH-A and PDI. These data demonstrate a possible response to the combined insult that is significantly different than either treatment alone, making them candidates for further study as potential biomarkers. Many of the proteins found in this study are currently recognized as biomarkers of disease processes including α-enolase which is found to be increased in many tumors; S100A9 has been found as a serum component after irradiation; and LDH, where a change in the usual LDH isozyme spectrum is indicative of ischemia, radiation treatment or cancer [37-42]. The identification of biomarkers in conjunction with changing isozyme spectra that are unique to a combination of environmental toxicants may lead to novel detection panels for suspected environmental toxicant exposures. With these findings, we have begun the process of identifying potential biomarkers of these types of combined exposures.

Acknowledgments

We would like to acknowledge that the first and second authors have made equal contributions to this work. We would like to thank Rebekah Woolsey at the Nevada Proteomics Center for her technical expertise and Karen Kalanetra for her help with manuscript preparation. This work was supported by grants from a Campus Laboratory Collaboration Grant 2003-2004 from UCOP (ZG), the Air Force Office of Scientific Research FA9550-06-1-0132 and FA9550-07-1-0146 (ZG, SB, and DMR), National Cancer Institute P30 CA093373-04 (DMR), NHGRI R01-HG003352 (DMR), NIEHS P42-ES04699 (DMR), UC Davis Health Systems (DMR) and the U.S. Department of Energy Office of Biological and Environmental Research, DE-FG02-01ER63237 and DE-FG02-07ER64341 (DMR, ZG), Nevada Proteomics Center NIH Grant Number P20 RR-016464 from the INBRE Program of the National Center for Research Resources.

Abbreviations

As, sodium arsenite; CaM, calmodulin; E-FABP, epidermal fatty acid-binding protein; HINT-1, histidine triad nucleotide-binding protein 1; HSP27, heat shock protein 27; IR, ionizing radiation; LDH-A, lactate dehydrogenase A; LDIR, low dose ionizing radiation; PDI, protein disulfide isomerase precursor.

References

1. Alavanja MC. Biologic damage resulting from exposure to tobacco smoke and from radon: implication for preventive interventions. Oncogene 2002;21:7365–7375. [PubMed: 12379879]
2. Hertz-Picciotto I, Smith AH, Holtzman D, Lipsett M, Alexeeff G. Synergism between occupational arsenic exposure and smoking in the induction of lung cancer. Epidemiology 1992;3:23–31. [PubMed: 1554806]
3. Hall EJ, Wuu CS. Radiation-induced second cancers: the impact of 3D-CRT and IMRT. Int J Radiat Oncol Biol Phys 2003;56:83–88. [PubMed: 12694826]
4. Tallman MS, Andersen JW, Schiffer CA, Appelbaum FR, et al. All-trans-retinoic acid in acute promyelocytic leukemia. N Engl J Med 1997;337:1021–1028. [PubMed: 9321529]
5. Ahsan H, Chen Y, Parvez F, Zablotska L, et al. Arsenic exposure from drinking water and risk of premalignant skin lesions in Bangladesh: baseline results from the Health Effects of Arsenic Longitudinal Study. Am J Epidemiol 2006;163:1138–1148. [PubMed: 16624965]
6. Yu HS, Liao WT, Chai CY. Arsenic carcinogenesis in the skin. J Biomed Sci 2006;13:657–666. [PubMed: 16807664]
7. Kitchin KT. Recent advances in arsenic carcinogenesis: modes of action, animal model systems, methylated arsenic metabolites. Toxicol Appl Pharmacol 2001;172:249–261. [PubMed: 11312654]
8. Klein CB, Leszczynska J, Hickey C, Rossman TG. Further evidence against a direct genotoxic mode of action for arsenic-induced cancer. Toxicol Appl Pharmacol 2007;222:289–297. [PubMed: 17316729]
9. Lau AT, He QY, Chiu JF. A proteome analysis of the arsenite response in cultured lung cells: evidence for in vitro oxidative stress-induced apoptosis. Biochem J 2004;382:641–650. [PubMed: 15175009]

10. Reichard JF, Schnekenburger M, Puga A. Long term low-dose arsenic exposure induces loss of DNA methylation. Biochem Biophys Res Commun 2007;352:188–192. [PubMed: 17107663]
11. Valko M, Rhodes CJ, Moncol J, Izakovic M, Mazur M. Free radicals, metals and antioxidants in oxidative stress-induced cancer. Chem Biol Interact 2006;160:1–40. [PubMed: 16430879]
12. Hamadeh HK, Trouba KJ, Amin RP, Afshari CA, Germolec D. Coordination of altered DNA repair and damage pathways in arsenite-exposed keratinocytes. Toxicol Sci 2002;69:306–316. [PubMed: 12377979]
13. Vogt BL, Rossman TG. Effects of arsenite on p53, p21 and cyclin D expression in normal human fibroblasts -- a possible mechanism for arsenite's comutagenicity. Mutat Res 2001;478:159–168. [PubMed: 11406180]
14. Schwartz JL. Variability: the common factor linking low dose-induced genomic instability, adaptation and bystander effects. Mutat Res 2007;616:196–200. [PubMed: 17145066]
15. Cook JA, Gius D, Wink DA, Krishna MC, et al. Oxidative stress, redo., and the tumor microenvironment. Semin Radiat Oncol 2004;14:259–266. [PubMed: 15254869]
16. Tubiana M, Aurengo A, Averbeck D, Masse R. The debate on the use of linear no threshold for assessing the effects of low doses. J Radiol Prot 2006;26:317–324. [PubMed: 16926474]
17. Andrew AS, Bernardo V, Warnke LA, Davey JC, et al. Exposure to arsenic at levels found inU.S. drinking water modifies expression in the mouse lung. Toxicol Sci 2007;100:75–87. [PubMed: 17682005]
18. Schoen A, Beck B, Sharma R, Dube E. Arsenic toxicity at low doses: epidemiological and mode of action considerations. Toxicol Appl Pharmacol 2004;198:253–267. [PubMed: 15276404]
19. Chen G, Gharib TG, Huang CC, Taylor JM, et al. Discordant protein and mRNA expression in lung adenocarcinomas. Mol Cell Proteomics 2002;1:304–313. [PubMed: 12096112]
20. Gygi SP, Rochon Y, Franza BR, Aebersold R. Correlation between protein and mRNA abundance in yeast. Mol Cell Biol 1999;19:1720–1730. [PubMed: 10022859]
21. Gottschalg E, Moore NE, Ryan AK, Travis LC, et al. Phenotypic anchoring of arsenic and cadmium toxicity in three hepatic-related cell systems reveals compound- and cell-specific selective up-regulation of stress protein expression: implications for fingerprint profiling of cytotoxicity. Chem Biol Interact 2006;161:251–261. [PubMed: 16729991]
22. Moore LE, Pfeiffer R, Warner M, Clark M, et al. Identification of biomarkers of arsenic exposure and metabolism in urine using SELDI technology. J Biochem Mol Toxicol 2005;19:176. [PubMed: 15977200]
23. Lee C, Lee YM, Rice RH. Human epidermal cell protein responses to arsenite treatment in culture. Chem Biol Interact 2005;155:43–54. [PubMed: 15899475]
24. Rosenfeld J, Capdevielle J, Guillemot JC, Ferrara P. In-gel digestion of proteins for internal sequence analysis after one- or two-dimensional gel electrophoresis. Anal Biochem 1992;203:173–179. [PubMed: 1524213]
25. Rocke DM. Design and analysis of experiments with high throughput biological assay data. Semin Cell Dev Biol 2004;15:703–713. [PubMed: 15561590]
26. Wright GW, Simon RM. A random variance model for detection of differential gene expression in small microarray experiments. Bioinformatics 2003;19:2448–2455. [PubMed: 14668230]
27. Benjamini Y, Hochberg Y. Controlling the False Discovery Rate: A Practical and Powerful Approach to Multiple Testing. Journal of the Royal Statistical Society. Series B (Methodological) 1995;57:289–300.
28. Ivanov VN, Zhou H, Hei TK. Sequential treatment by ionizing radiation and sodium arsenite dramatically accelerates TRAIL-mediated apoptosis of human melanoma cells. Cancer Res 2007;67:5397–5407. [PubMed: 17545621]
29. Bernstam L, Lan CH, Lee J, Nriagu JO. Effects of arsenic on human keratinocytes: morphological, physiologica., and precursor incorporation studies. Environ Res 2002;89:220–235. [PubMed: 12176006]
30. Franco N, Lamartine J, Frouin V, Le Minter P, et al. Low-dose exposure to gamma rays induces specific gene regulations in normal human keratinocytes. Radiat Res 2005;163:623–635. [PubMed: 15913394]

31. Ding LH, Shingyoji M, Chen F, Hwang JJ, et al. Gene expression profiles of normal human fibroblasts after exposure to ionizing radiation: a comparative study of low and high doses. Radiat Res 2005;164:17–26. [PubMed: 15966761]
32. Berglund SR, Rocke DM, Dai J, Schwietert CW, et al. Transient genome-wide transcriptional response to low-dose ionizing radiation in vivo in humans. Int J Radiat Oncol Biol Phys 2008;70:229–234. [PubMed: 17996396]
33. Goldberg Z, Rocke DM, Schwietert C, Berglund SR, et al. Human in vivo dose-response to controlled, low-dose low linear energy transfer ionizing radiation exposure. Clin Cancer Res 2006;12:3723–3729. [PubMed: 16778099]
34. Yang F, Stenoien DL, Strittmatter EF, Wang J, et al. Phosphoproteome profiling of human skin fibroblast cells in response to low- and high-dose irradiation. J Proteome Res 2006;5:1252–1260. [PubMed: 16674116]
35. Zhang B, Su YP, Ai GP, Liu XH, et al. Differentially expressed proteins of gamma-ray irradiated mouse intestinal epithelial cells by two-dimensional electrophoresis and MALDI-TOF mass spectrometry. World J Gastroenterol 2003;9:2726–2731. [PubMed: 14669322]
36. Prasad SC, Soldatenkov VA, Kuettel MR, Thraves PJ, et al. Protein changes associated with ionizing radiation-induced apoptosis in human prostate epithelial tumor cells. Electrophoresis 1999;20:1065–1074. [PubMed: 10344286]
37. Ewald N, Toepler M, Akinci A, Kloer HU, et al. [Pyruvate kinase M2 (tumor M2-PK) as a screening tool for colorectal cancer (CRC). A review of current published data]. Z Gastroenterol 2005;43:1313–1317. [PubMed: 16315127]
38. Ishiguro Y, Kato K, Ito T, Horisawa M, Nagaya M. Enolase isozymes as markers for differential diagnosis of neuroblastoma, rhabdomyosarcom., and Wilms' tumor. Gann 1984;75:53–60. [PubMed: 6327451]
39. Katayama M, Nakano H, Ishiuchi A, Wu W, et al. Protein pattern difference in the colon cancer cell lines examined by two-dimensional differential in-gel electrophoresis and mass spectrometry. Surg Today 2006;36:1085–1093. [PubMed: 17123137]
40. Nagasue N. Changes in lactic dehydrogenase isoenzymes after hepatic artery ligation in patients with hepatic carcinoma. Gastroenterol Jpn 1975;10:150–156. [PubMed: 185117]
41. Pandit MK, Joshi BH, Patel PS, Chitnis KE, Balar DB. Efficacy of serum lactate dehydrogenase and its isozymes in monitoring the therapy in patients with acute leukemia. Indian J Pathol Microbiol 1990;33:41–47. [PubMed: 2394475]
42. Sewell DA, Yuan CX, Robertson E. Proteomic signatures in laryngeal squamous cell carcinoma. ORL J Otorhinolaryngol Relat Spec 2007;69:77–84. [PubMed: 17127822]

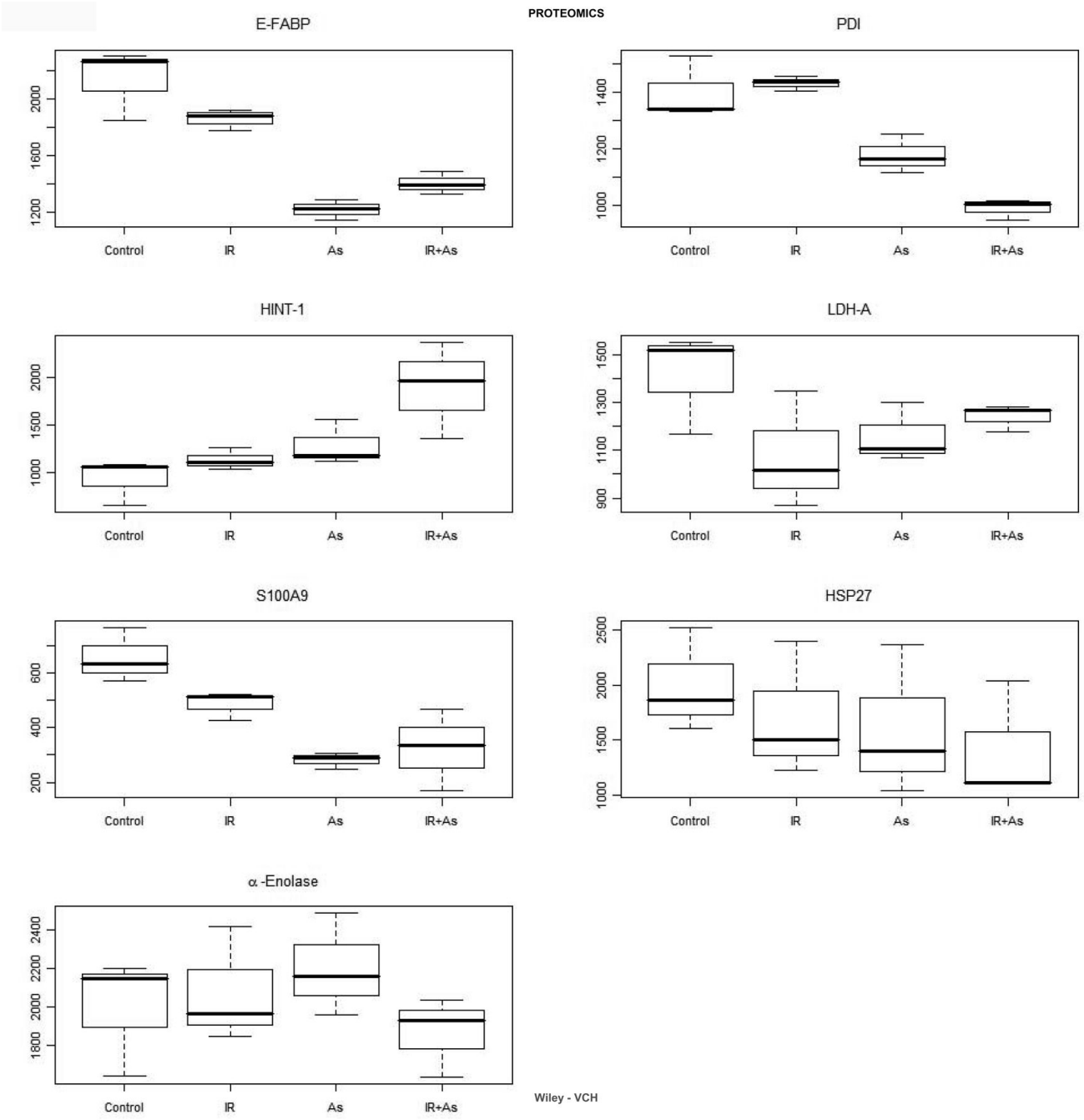

Figure 1.

Immunoblot data of proteins identified by MS/MS. Immunoblots were performed for each selected protein and density (intensity per mm2) was calculated on a ChemiDoc system (BioRad, CA). This figure shows boxplots for each analyte for which there was at least one significant effect by ANOVA. Significant effects for these analytes are shown in Table 2.

Table 1

Protein identification. Proteins identified from mass spectrometry and tandem mass spectrometry. Fields include: spot number as displayed in figure 1, protein name, accession number from CDScombined database (Celera Discovery System v. KBMS3.2.20040119), MASCOT protein score, MASCOT ion score, protein and ion score confidence indices, species of protein hit, total amino acid sequence coverage, protein molecular weight, pI, and peptide count. Also shown are the matched peptides and corresponding masses, mass errors, sequences and number of unmatched sequences if fewer than two peptides were confirmed by CID. Peptides analyzed by tandem mass spectrometry display ion scores and confidence indices.

Spot Number	Protein Name	Accession Number	Protein Score	Total Ion Score	Total Ion C. I. %	Protein Score C.I.%	Species	% AA Seq. Coverage	Protein MW	Protein pI	Peptide Count
795	Pyruvate kinase, M1/M2 isozyme (EC 2.7.1.40) (Pyruvate kinase muscle isozyme) (Cytosolic thyroid hormone)	spt|P14618	77	25	86.618	97.301	Homo sapiens	16	57769	7.95	11

Peptide Information

Calc. Mass	Obsrv. Mass	± da	± ppm	Start Seq.	End Seq.	Sequence	Ion Score	C. I. %	Modification	# unmatched
717.4141	717.4005	-0.0136	-19	166	172	VVEVGSK				54
730.4457	730.4366	-0.0091	-12	256	262	VLGEKGK				
731.3934	731.3998	0.0064	9	224	229	DIQDLK				
787.4209	787.4111	-0.0098	-12	461	466	QAHLYR				
912.4533	912.4691	0.0158	17	247	254	ASDVHEVR				
953.4799	953.4738	-0.0061	-6	270	277	IENHEGVR				
995.4978	995.4794	-0.0184	-18	489	497	VNFAMNVGK			Oxidation (M)[5]	
1019.5156	1019.4958	-0.0198	-19	367	375	GDYPLEAVR				
1040.5483	1040.5513	0.003	3	247	255	ASDVHEVRK				
1197.6475	1197.626	-0.0215	-18	32	42	LDIDSPPITAR				
1359.705	1359.6838	-0.0212	-16	43	55	NTGIICTIGPASR			Carbamidomethyl (C)[6]	

Spot Number	Protein Name	Accession Number	Protein Score	Total Ion Score	Total Ion C. I. %	Protein Score C.I.%	Species	% AA Seq. Coverage	Protein MW	Protein pI	Peptide Count
853	Thyroid hormone binding protein precursor (protein disulfide isomerase precursor) (prolyl 4-hydroxylase, beta subunit precursor)	gb|AAA61169	128	80	100	100	Homo sapiens	18	57068.7	4.82	10

Peptide Information

Calc. Mass	Obsrv. Mass	± da	± ppm	Start Seq.	End Seq.	Sequence	Ion Score	C. I. %	Modification	# unmatched
763.4348	763.4481	0.0133	17	248	254	IFGGEIK				55
808.4562	808.4619	0.0057	7	462	468	TLDGFKK				
862.4668	862.4716	0.0048	6	58	65	ALAPEYAK				
910.4417	910.4497	0.008	9	445	452	FFPASADR				
928.525	928.5292	0.0042	5	437	444	VHSFPTLK				
962.4512	962.4545	0.0033	3	339	345	ITEFCHR			Carbamidomethyl (C)[5]	
1002.5577	1002.558	0.0003	0	70	78	LKAEGSEIR				
1066.5164	1066.5112	-0.0052	-5	453	461	TVIDYNGER				
1451.7013	1451.6896	-0.0117	-8	327	338	YKPESEELTAER				
1780.8348	1780.8119	-0.0229	-13	82	97	VDATEESDLAQQYGVR				

Spot Number	Protein Name	Accession Number	Protein Score	Total Ion Score	Total Ion C. I. %	Protein Score C.I.%	Species	% AA Seq. Coverage	Protein MW	Protein pI	Peptide Count
1017	Annexin A11 (Annexin XI) (Calcyclin-associated annexin 50)(CAP-50)	spt|P50995	221	123	100	100	Homo sapiens	27	54355.1	7.53	14

Peptide Information

Calc. Mass	Obsrv. Mass	± da	± ppm	Start Seq.	End Seq.	Sequence	Ion Score	C. I. %	Modification	
748.4133	748.4154	0.0021	3	440	445	LNKAMR			Oxidation (M)[5]	
789.4902	789.4913	0.0011	1	265	271	TILALMK				
831.457	831.4673	0.0103	12	321	327	TLEEAIR				
959.5519	959.5665	0.0146	15	320	327	KTLEEAIR				
976.5825	976.5814	-0.0011	-1	236	243	QQILLSFK				
1034.465	1034.4786	0.0136	13	328	336	SDTSGHFQR				
1052.516	1052.5264	0.0104	10	431	439	NTPAFFAER	44	99.702		Confirmed by CID
1336.6128	1336.6226	0.0098	7	360	371	DAQELYAAGENR	51	99.95		Confirmed by CID
1446.7488	1446.7614	0.0126	9	389	400	AHLVAVFNEYQR				

1453.7256	1453.7286	0.003	2	428	439	CLKNTPAFFAER	Carbamidomethyl (C)[1]
1696.8323	1696.8431	0.0108	6	372	386	LGTDESKFNAVLCSR	Carbamidomethyl (C)[13]
1703.8633	1703.8745	0.0112	7	287	302	GVGTDEACLIEILASR	Carbamidomethyl (C)[8]
1738.8064	1738.8142	0.0078	4	215	230	GFGTDEQAIIDCLGSR	Carbamidomethyl (C)[12]
1813.8351	1813.8444	0.0093	5	480	495	SLYHDISGDTSGDYRK	

Spot Number	Protein Name	Accession Number	Protein Score	Total Ion Score	Total Ion C. I. %	Protein Score C.I.%	Species	% AA Seq. Coverage	Protein MW	Protein pI	Peptide Count
1096	Enolase 1 (α-enolase)	rf|NP_001419.	539	262	100	100	Homo sapiens	73	47139.3	7.01	26

Peptide Information

Calc. Mass	Obsrv. Mass	± da	± ppm	Start Seq.	End Seq.	Sequence	Ion Score	C. I. %	Modification
704.4089	704.4009	-0.008	-11	127	132	GVPLYR			
766.3729	766.3828	0.0099	13	10	15	EIFDSR			
806.4518	806.4534	0.0016	2	407	412	YNQLLR			
959.5421	959.5441	0.002	2	427	434	NFRNPLAK	45	99.8	Confirmed by CID
1007.5012	1007.5017	0.0005	0	336	343	SCNCLLLK			Carbamidomethyl (C)[2,4]
1143.6156	1143.6161	0.0005	0	184	193	IGAEVYHNLK			
1259.7106	1259.7244	0.0138	11	121	132	AGAVEKGVPLYR			
1406.7162	1406.7166	0.0004	0	16	28	GNPTVEVDLFTSK			
1425.7261	1425.7271	0.001	1	270	281	YISPDQLADLYK			
1525.7693	1525.7821	0.0128	8	359	372	LAQANGWGVMVSHR	48	99.904	Confirmed by CID
1540.7828	1540.7863	0.0035	2	240	253	VVIGMDVAASEFFR			
1541.7642	1541.7775	0.0133	9	359	372	LAQANGWGVMVSHR			
1556.7777	1556.7732	-0.0045	-3	240	253	VVIGMDVAASEFFR			Oxidation (M)[5]
1597.906	1597.9109	0.0049	3	184	197	IGAEVYHNLKNVIK			
1633.8214	1633.827	0.0056	3	344	358	VNQIGSVTESLQACK			Carbamidomethyl (C)[14]
1690.985	1690.989	0.004	2	65	80	AVEHINKTIAPALVSK			
1691.8962	1691.9104	0.0142	8	407	420	YNQLLRIEEELGSK			
1804.9438	1804.9542	0.0104	6	33	50	AAVPSGASTGIYEALELR			
1907.9869	1908	0.0131	7	163	179	LAMQEFMILPVGAANFR	83	100	Confirmed by CID
1923.9819	1923.9922	0.0103	5	163	179	LAMQEFMILPVGAANFR	62	99.996	Oxidation (M)[3] Confirmed by CID
1939.9768	1939.9871	0.0103	5	163	179	LAMQEFMILPVGAANFR			
2033.0549	2033.0754	0.0205	10	307	326	FTASAGIQVVGDDLTVTNPK			
2154.0713	2154.0823	0.011	5	10	28	EIFDSRGNPTVEVDLFTSK	32	95.649	Confirmed by CID
2176.0742	2176.0864	0.0122	6	234	253	AGYTDKVVIGMDVAASEFFR			
2189.156	2189.1685	0.0125	6	307	327	FTASAGIQVVGDDLTVTNPKR			
2192.0691	2192.1094	0.0403	18	234	253	AGYTDKVVIGMDVAASEFFR			Oxidation (M)[11]
2277.1357	2277.1489	0.0132	6	33	54	AAVPSGASTGIYEALELRDNDK			
2353.1592	2353.1702	0.011	5	373	394	SGETEDTFIADLVVGLCTGQIK			Carbamidomethyl (C)[17]
2743.3784	2743.3887	0.0103	4	203	228	DATNVGDEGGFAPNILENKEGLELLK			
2985.394	2985.3994	0.0054	2	282	306	SFIKDYPVVSIEDPFDQDDWGAWQK			
3011.5696	3011.5767	0.0071	2	133	162	HIADLAGNSEVILPVPAFNVINGGSHAGNK			

Spot Number	Protein Name	Accession Number	Protein Score	Total Ion Score	Total Ion C. I. %	Protein Score C.I.%	Species	% AA Seq. Coverage	Protein MW	Protein pI	Peptide Count
1573	Lactate dehydrogenase A	rf|NP_005557.	119	76	100	100	Homo sapiens	21	36665.4	8.44	8

Peptide Information

Calc. Mass	Obsrv. Mass	± da	± ppm	Start Seq.	End Seq.	Sequence	Ion Score	C. I. %	Modification	# unmatched
734.4195	734.426	0.0065	9	113	118	NVNIFK				58
742.457	742.4594	0.0024	3	107	112	LNLVQR				
913.5828	913.5876	0.0048	5	91	99	LVIITAGAR				
929.5818	929.5841	0.0023	2	119	126	FIIPNVVK				
1027.5605	1027.5479	-0.0126	-12	270	278	VHPVSTMIK			Oxidation (M)[7]	
1118.5841	1118.5861	0.002	2	319	328	SADTLWGIQK				
1134.5637	1134.573	0.0093	8	306	315	VTLTSEEEAR				

	1248.6001	1248.6068	0.0067	5	158	169	VIGSGCNLDSAR					Carbamidomethyl (C)[6]				
Spot Number	**Protein Name**						**Accession Number**	**Protein Score**	**Total Ion Score**	**Total Ion C. I. %**	**Protein Score C.I.%**	**Species**	**% AA Seq. Coverage**	**Protein MW**	**Protein pI**	**Peptide Count**
1968	Heat shock 27 kDa protein (HSP 27) (Stress-responsive protein 27) (SRP27) (Estrogen-regulated 24 kD protein)						spt|P04792	212	133	100	100	Homo sapiens	43	22768.5	5.98	9
	Peptide Information															
	Calc. Mass	**Obsrv. Mass**	**± da**	**± ppm**	**Start Seq.**	**End Seq.**	**Sequence**			**Ion Score**	**C. I. %**	**Modification**				
	831.5086	831.5093	0.0007	1	6	12	VPFSLLR									
	941.505	941.5215	0.0165	18	189	198	AQLGGPEAAK									
	961.4526	961.4537	0.0011	1	13	20	GPSWDPFR									
	987.6097	987.6163	0.0066	7	5	12	RVPFSLLR									
	1075.5742	1075.5763	0.0021	2	80	89	QLSSGVSEIR									
	1104.5068	1104.5123	0.0055	5	128	136	QDEHGYISR									
	1163.6207	1163.6315	0.0108	9	28	37	LFDQAFGLPR			58	99.988			Confirmed by CID		
	1783.9225	1783.9335	0.011	6	97	112	VSLDVNHFAPDELTVK									
	1905.9916	1905.9955	0.0039	2	172	188	LATQSNEITIPVTFESR			61	99.994			Confirmed by CID		
Spot Number	**Protein Name**						**Accession Number**	**Protein Score**	**Total Ion Score**	**Total Ion C. I. %**	**Protein Score C.I%**	**Species**	**% AA Seq. Coverage**	**Protein MW**	**Protein pI**	**Peptide Count**
2466	Calmodulin						spt|P02593	213	173	100	100	Homo sapiens	50	16695.8	4.09	5
	Peptide Information															
	Calc. Mass	**Obsrv. Mass**	**± da**	**± ppm**	**Start Seq.**	**End Seq.**	**Sequence**			**Ion Score**	**C. I. %**	**Modification**				
	805.4236	805.4288	0.0052	6	31	37	ELGTVMR									
	1596.7136	1596.72	0.0064	4	78	90	DTDSEEEIREAFR									
	1754.8707	1754.8773	0.0066	4	91	106	VFDKDGNGYISAAELR			136	100			Confirmed by CID		
	1844.8912	1844.8918	0.0006	0	14	30	EAFSLFDKDGDGTITTK			37	98.993			Confirmed by CID		
	2490.0798	2490.0576	-0.0222	-9	127	148	EADIDGDGQVNYEEFVQMMTAK									
	2506.0747	2506.0603	-0.0144	-6	127	148	EADIDGDGQVNYEEFVQMMTAK					Oxidation (M)[18]				
Spot Number	**Protein Name**						**Accession Number**	**Protein Score**	**Total Ion Score**	**Total Ion C. I. %**	**Protein Score C.I.%**	**Species**	**% AA Seq. Coverage**	**Protein MW**	**Protein pI**	**Peptide Count**
2529	Peptidyl-prolyl cis-trans isomerase A (EC 5.2.1.8) (Cyclophilin A)(PPIase)(Rotamase) (Cyclosporin A-binding protein)						spt|P05092	197	139	100	100	Homo sapiens	50	17869.8	7.82	7
	Peptide Information															
	Calc. Mass	**Obsrv. Mass**	**± da**	**± ppm**	**Start Seq.**	**End Seq.**	**Sequence**			**Ion Score**	**C. I. %**	**Modification**				
	1154.5728	1154.5836	0.0108	9	82	90	FEDENFILK									
	1247.63	1247.6351	0.0051	4	154	164	KITIADCGQLE					Carbamidomethyl (C)[7]				
	1379.757	1379.7665	0.0095	7	19	30	VSFELFADKVPK			56	99.985			Confirmed by CID		
	1505.745	1505.7593	0.0143	9	131	143	VKEGMNIVEAMER									
	1521.74	1521.7468	0.0068	4	131	143	VKEGMNIVEAMER					Oxidation (M)[5]				
	1598.7454	1598.7604	0.015	9	55	68	IIPGFMCQGGDFTR			42	99.637	Carbamidomethyl (C)[7]		Confirmed by CID		
	1614.7402	1614.7517	0.0115	7	55	68	IIPGFMCQGGDFTR					Carbamidomethyl (C)[7], Oxidation (M)[6]				
	1831.9113	1831.918	0.0067	4	76	90	SIYGEKFEDENFILK			41	99.434			Confirmed by CID		
	1946.0017	1946.0099	0.0082	4	1	18	VNPTVFFDIAVDGEPLGR									
Spot Number	**Protein Name**						**Accession Number**	**Protein Score**	**Total Ion Score**	**Total Ion C. I. %**	**Protein Score C.I.%**	**Species**	**% AA Seq. Coverage**	**Protein MW**	**Protein pI**	**Peptide Count**
2585	R33729_1 (Fragment)						trm|O75256	169	137	100	100	Homo sapiens	47	11325.7	7.03	4
	Peptide Information															
	Calc. Mass	**Obsrv. Mass**	**± da**	**± ppm**	**Start Seq.**	**End Seq.**	**Sequence**			**Ion Score**	**C. I. %**	**Modification**				
	1154.6428	1154.6522	0.0094	8	72	82	TAVAHRPGAFK									
	1196.5986	1196.5968	-0.0018	-2	27	35	SYLYFTQFK			62	99.996			Confirmed by CID		
	1332.614	1332.6141	0.0001	0	40	51	GAEIEYAMAYSK									
	1348.6089	1348.6102	0.0013	1	40	51	GAEIEYAMAYSK					Oxidation (M)[8]				
	1750.8745	1750.8795	0.005	3	57	71	ESDVPLKTEEFEVTK			59	99.991			Confirmed by CID		

Spot Number	Protein Name	Accession Number	Protein Score	Total Ion Score	Total Ion C. I. %	Protein Score C.I.%	Species	% AA Seq. Coverage	Protein MW	Protein pI	Peptide Count
2611	Fatty acid-binding protein, epidermal (E-FABP) (Psoriasis-associated fatty acid-binding protein homolog)	spt|Q01469	342	276	100	100	Homo sapiens	64	15154.5	6.6	7

Peptide Information

Calc. Mass	Obsrv. Mass	± da	± ppm	Start Seq.	End Seq.	Sequence	Ion Score	C. I. %	Modification	
889.376	889.3785	0.0025	3	18	24	GFDEYMK				
905.3709	905.3723	0.0014	2	18	24	GFDEYMK				
927.5621	927.5629	0.0008	1	25	33	ELGVGIALR	54	99.983		Confirmed by CID
1271.5936	1271.5996	0.006	5	62	72	TTQFSCTLGEK	55	99.987	Carbamidomethyl (C)[6]	Confirmed by CID
1694.8022	1694.7999	-0.0023	-1	116	129	LVVECVMNNVTCTR	89	100	Carbamidomethyl (C)[5,12]	Confirmed by CID
1710.7971	1710.8018	0.0047	3	116	129	LVVECVMNNVTCTR	52	99.967	Carbamidomethyl (C)[5,12], Oxidation (M)[	Confirmed by CID
1767.7897	1767.7905	0.0008	0	35	50	MGAMAKPDCIITCDGK	50	99.958	Carbamidomethyl (C)[9,13]	Confirmed by CID
1783.7845	1783.7753	-0.0092	-5	35	50	MGAMAKPDCIITCDGK				
2278.0293	2278.0212	-0.0081	-4	62	81	TTQFSCTLGEKFEETTADGR			Carbamidomethyl (C)[6]	
2434.1091	2434.0994	-0.0097	-4	83	103	TQTVCNFTDGALVQHQEWDGK			Carbamidomethyl (C)[5]	

Spot Number	Protein Name	Accession Number	Protein Score	Total Ion Score	Total Ion C. I. %	Protein Score C.I.%	Species	% AA Seq. Coverage	Protein MW	Protein pI	Peptide Count
2640	Fatty acid-binding protein, epidermal (Psoriasis-associated E-FABP)	spt|Q01469	182	81	100	100	Homo sapiens	58	15154.5	6.6	6

Peptide Information

Calc. Mass	Obsrv. Mass	± da	± ppm	Start Seq.	End Seq.	Sequence	Ion Score	C. I. %	Modification	# unmatched	
889.376	889.3734	-0.0026	-3	18	24	GFDEYMK				53	
903.5046	903.5063	0.0017	2	11	17	WRLVDSK					
927.5621	927.5521	-0.01	-11	25	33	ELGVGIALR					
1055.6571	1055.6429	-0.0142	-13	25	34	ELGVGIALRK					
1694.8022	1694.7769	-0.0253	-15	116	129	LVVECVMNNVTCTR	81	100	Carbamidomethyl (C)[5,12]		Confirmed by CID
1710.7682	1710.7815	0.0133	8	35	50	MGAMAKPDCIITCDGK			Carbamidomethyl (C)[9]		

Spot Number	Protein Name	Accession Number	Protein Score	Total Ion Score	Total Ion C. I. %	Protein Score C.I.%	Species	% AA Seq. Coverage	Protein MW	Protein pI	Peptide Count
2671	Profilin I	spt|P07737	112	63	99.998	100	Homo sapiens	55	14913.5	8.48	6

Peptide Information

Calc. Mass	Obsrv. Mass	± da	± ppm	Start Seq.	End Seq.	Sequence	Ion Score	C. I. %	Modification	# unmatched	
1151.6531	1151.6593	0.0062	5	116	126	EGVHGGLINKK				60	
1166.5082	1166.5278	0.0196	17	127	135	CYEMASHLR	44	99.866	Carbamidomethyl (C)[1]		Confirmed by CID
1322.6093	1322.6267	0.0174	13	127	136	CYEMASHLRR			Carbamidomethyl (C)[1]		
1470.7587	1470.7845	0.0258	18	56	69	SSFYVNGLTLGGQK					
1625.7476	1625.766	0.0184	11	75	88	DSLLQDGEFSMDLR					
1915.0647	1915.0964	0.0317	17	38	55	TFVNITPAEVGVLVGKDR					

Spot Number	Protein Name	Accession Number	Protein Score	Total Ion Score	Total Ion C. I. %	Protein Score C.I.%	Species	% AA Seq. Coverage	Protein MW	Protein pI	Peptide Count
2686	Calgranulin B (Migration inhibitory factor-related protein 14)(Leukocyte L1 complex) -	spt|P06702	473	391	100	100	Homo sapiens	74	13233.5	5.71	8

Peptide Information

Calc. Mass	Obsrv. Mass	± da	± ppm	Start Seq.	End Seq.	Sequence	Ion Score	C. I. %	Modification	
877.4777	877.4815	0.0038	4	44	50	DLQNFLK	43	99.688		Confirmed by CID
971.4944	971.499	0.0046	5	86	93	LTWASHEK				
1005.5727	1005.5754	0.0027	3	44	51	DLQNFLKK	52	99.964		Confirmed by CID
1455.7227	1455.7358	0.0131	9	26	38	LGHPDTLNQGEFK	109	100		Confirmed by CID
1742.8265	1742.8383	0.0118	7	58	72	VIEHIMEDLDTNADK				
1806.9385	1806.9559	0.0174	10	11	25	NIETIINTFHQYSVK	94	100		Confirmed by CID
1953.0188	1953.0376	0.0188	10	26	42	LGHPDTLNQGEFKELVR	95	100		Confirmed by CID
2175.9624	2175.9773	0.0149	7	94	114	MHEGDEGPGHHHKPGLGEGTP				

Spot Number	Protein Name	Accession Number	Protein Score	Total Ion Score	Total Ion C. I. %	Protein Score C.I.%	Species	% AA Seq. Coverage	Protein MW	Protein pI	Peptide Count
2687	Histidine triad nucleotide-binding protein 1 (HINT-1) (Adenosine 5 monophosphoramidase) (PKCI-1)	spt|P49773	91	62	99.996	99.879	Homo sapiens	22	13662	6.46	4

Peptide Information

Calc. Mass	Obsrv. Mass	± da	± ppm	Start Seq.	End Seq.	Sequence	Ion Score	C. I. %	Modification	# unmatched	
961.4771	961.4674	-0.0097	-10	83	91	CAADLGLNK			Carbamidomethyl (C)[1]	61	
1032.5507	1032.55	-0.0007	-1	82	91	KCAADLGLNK					
1337.663	1337.6392	-0.0238	-18	83	94	CAADLGLNKGYR	35	98.049	Carbamidomethyl (C)[1]		Confirmed by CID
1416.7594	1416.7352	-0.0242	-17	7	20	AQVARPGGDTIFGK					

Table 2

Significant effects in the ANOVA of the western blot analysis. The p-value is given for all effects significant at the 0.05 level. The (↑) symbol in the ionizing radiation (IR) or arsenic (As) column indicates that the given protein is up regulated upon treatment with the respective toxicant, and the (↓) symbol indicates down regulation. For the IR*As interaction, the (+) symbol indicates that the protein expression is greater than would have been expected from the two stimuli independently, and (−) indicates that the protein expression is less than would have been expected. In general, we can conclude that there has been evidence of an IR perturbation of protein expression if either the IR or the IR*As effect is significant, and that there has been evidence of an As perturbation if either the As or IR*As effect is significant. Thus 6 of the 11 proteins showed a reaction to IR, 8 of the 11 showed a reaction to As (including all that showed a reaction to IR), and 3 were inconclusive. The ANOVA was performed for all exposures, — indicates no significant change.

Protein	IR	Arsenic	IR*As
E-FABP	—	(↓) p=0.0001	(+) p=0.0158
↓-Enolase	—	—	(−) p=0.0151
HINT-1	(↓) p=0.0348	(↓) p=0.0095	—
HSP27	(↓) p=0.0135	(↓) p=0.0024	—
LDH-A	—	—	(+) p=0.0435
PDI	—	(↓) p=0.0001	(−) p=0.0268
S100A9	—	(↓) p=0.0010	—
Annexin XI	—	—	—
Cyclophilin A	—	—	—
Profilin	—	—	—
Pyruvate Kinase, M	—	—	—